FT-EPR Study of Methyl Radicals Photogenerated from [Ru(Me)(SnPh$_3$)(CO)$_2$(iPr-DAB)] and [Pt(Me)$_4$(iPr-DAB)]: An Example of a Strong Excitation Wavelength Dependent CIDEP Effect

Joris van Slageren,[†] Débora M. Martino,[‡,§] Cornelis J. Kleverlaan,[†] Alejandro P. Bussandri,[‡] Hans van Willigen,*[,‡] and Derk J. Stufkens[†]

Institute of Molecular Chemistry, Universiteit van Amsterdam, Nieuwe Achtergracht 166, NL-1018 WV Amsterdam, The Netherlands, and Department of Chemistry, University of Massachusetts at Boston, Boston, Massachusetts 02125

Received: March 17, 2000; In Final Form: April 24, 2000

The photoinduced methyl radical formation from the title complexes [Ru(R)(SnPh$_3$)(CO)$_2$(iPr-DAB)] (R = CH$_3$, CD$_3$; iPr-DAB = *N*,*N*′-diisopropyl-1,4-diaza-1,3-butadiene) and [Pt(Me)$_4$(iPr-DAB)] was the subject of a detailed time-resolved Fourier transform EPR (FT-EPR) study. The FT-EPR spectra of the radicals show pronounced chemically induced dynamic electron polarization (CIDEP) effects due to the ST_0 and ST_{-1} radical pair mechanisms (RPM). The relative contributions of the two CIDEP mechanisms depend on solvent polarity and viscosity. In the case of the [Ru(R)(SnPh$_3$)(CO)$_2$(iPr-DAB)] complexes, the polarization pattern is also strongly excitation wavelength dependent. This effect is attributed to extremely fast reactions from different thermally nonequilibrated σ-bond-to-ligand charge transfer (SBLCT) excited states.

Introduction

Many studies have been made of the photochemical alkyl radical formation from transition metal[1−10] and main group metal[11−13] compounds with alkyl ligands. Alkyl radicals can be used as addition polymerization initiators[14] or reagents in organic synthesis.[15] Therefore these types of metal−alkyl compounds can be very useful in these fields.[16]

Detailed (time-resolved) spectroscopic studies revealed that in the case of the complexes [Re(R)(CO)$_3$(dmb)] (R = Me, Et, iPr; dmb = 4,4′-dimethyl-2,2′-bipyridine)[2−4] and [Ru(I)(R′)-(CO)$_2$(iPr-DAB)][5,17] (R′ = iPr, Bz; iPr-DAB = *N*,*N*′-diisopropyl-1,4-diaza-1,3-butadiene) radical formation proceeds through a metal−alkyl bond homolysis reaction from a σ-bond-to-ligand charge transfer (SBLCT) state. This reactive excited state is populated from an optically excited state that has predominant metal-to-ligand charge transfer (MLCT) character. In the case of [Ru(L$_1$)(L$_2$)(CO)$_2$(iPr-DAB)] (L$_1$, L$_2$ = alkyl group or metal fragment) and [Pt(Me)$_4$(iPr-DAB)], the lowest energy transition has SBLCT character. In these complexes, the SBLCT state is fairly stable and long-lived in the case of [Ru(SnPh$_3$)$_2$(CO)$_2$-(iPr-DAB)][18] but very reactive for [Ru(CH$_3$)(SnPh$_3$)(CO)$_2$-(iPr-DAB)] (**1H**) and [Pt(Me)$_4$(iPr-DAB)] (**2**).[1,6]

Our recent work has shown that Fourier transform EPR (FT-EPR) spectroscopy can be a very useful technique in studies of the mechanism of photoinduced radical formation from organometallic complexes.[2,19] Analysis of the chemically induced dynamic electron polarization (CIDEP) effects, which are caused by spin-selective photophysical and photochemical processes, gave insight into the dynamics of alkyl radical formation. FT-EPR studies showed that the radical formation occurs from a precursor with triplet character in these cases. Apart from our own studies, one other time-resolved EPR study in organometallic chemistry is known.[20]

Despite our successful application of the FT-EPR technique in the field of organometallic photochemistry, the remarkably strong dependence of CIDEP effects on the nature of ligands and solvent found in our earlier work were not fully understood. Here we present a detailed FT-EPR study of the (deuterated) methyl radical formation from the organometallic complexes [Ru(R)(SnPh$_3$)(CO)$_2$(iPr-DAB)] (R = CH$_3$, CD$_3$) (**1H** and **1D**, respectively) and [Pt(Me)$_4$(iPr-DAB)] (**2**). Of particular interest is the finding that the methyl radical spectra in the case of **1** display a *spin polarization pattern that is strongly dependent on excitation wavelength*. A preliminary account of this work has appeared in the literature.[21]

Experimental Section

The complexes [Ru(R)(SnPh$_3$)(CO)$_2$(iPr-DAB)] (R = CH$_3$, CD$_3$; iPr-DAB = *N*,*N*′-diisopropyl-1,4-diazabutadiene) (**1H** and **1D**, respectively)[22] and [Pt(Me)$_4$(iPr-DAB)] (**2**)[23] were synthesized according to literature procedures. Toluene, dichloromethane, methanol, 2-propanol, ethylene glycol, and 1,2-propane diol (Aldrich) were used as received.

FT-EPR measurements were performed with a home-built spectrometer.[24,25] The response of the sample to the $\pi/2$ microwave pulses was detected in quadrature with application of the CYCLOPS phase cycling routine. All measurements were performed at room temperature. Solutions of the complexes (ca. 1−2 mM) were freed of oxygen by purging with argon prior to and during measurements. The solutions were pumped through a quartz EPR flow cell held in the microwave cavity. The second or third harmonic of a Quanta Ray GCR12 Nd:YAG laser (∼20 mJ/pulse, 10 Hz) was used for excitation at 532 or 355 nm, a Lambda-Physik EMG103 MSC XeCl excimer laser for excitation at 308 nm (∼20 mJ, 10 Hz), and an excimer laser pumped dye laser (Lambda-Physik FL 3001, ∼2 mJ, 10 Hz) for

* Corresponding author. E-mail: hans.vanwilligen@umb.edu.
[†] Universiteit van Amsterdam.
[‡] University of Massachusetts at Boston.
[§] Present address: Physics Department, INTEC (CONICET) and FBCB, UNL, 3000 Santa Fe, Argentina.

10.1021/jp001032b CCC: $19.00
Published on Web 06/02/2000

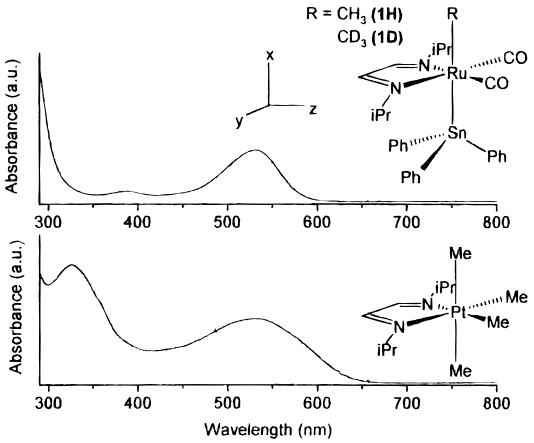

Figure 1. Schematic molecular structures and electronic absorption spectra of $[Ru(Me)(SnPh_3)(CO)_2(iPr\text{-}DAB)]$ (**1H**) and $[Pt(Me)_4(iPr\text{-}DAB)]$ (**2**) in toluene.

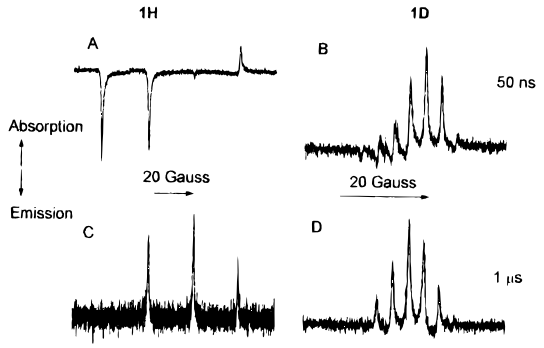

Figure 2. FT-EPR spectra of the methyl radicals produced by photoexcitation (532 nm) of ~1 mM $[Ru(R)(SnPh_3)(CO)_2(iPr\text{-}DAB)]$, R = CH_3 (**1H**, left) or CD_3 (**1D**, right), in toluene for short (50 ns) and long (1 μs) delay times. Note that the field range of the $CD_3^\bullet$ spectra is smaller than that of the $CH_3^\bullet$ spectra and that absorption peaks point up.

excitation at 440 nm. Unless noted otherwise, 400 FIDs (100 per phase) were averaged to obtain the spectra.

The time evolution of transient spectra was measured as follows. The FID produced by a $\pi/2$ (15 ns) microwave pulse was recorded for a series of delay times τ_d (10 ns to 5 μs) between laser and microwave pulses. Amplitudes, line widths, and phases of resonance peaks were derived from the FIDs with a LPSVD analysis routine.[26] Since the spectra of the methyl radicals cover a frequency range that far exceeds the bandwidth of the spectrometer, EPR spectra presented in the figures are assembled from FIDs obtained with a set of distinct field values. Spectra from the deuterated methyl radical were obtained at a single field setting. Spectral intensities were corrected for photochemical decomposition during the measurement. Corrections for the variation in signal intensity with change in frequency offset were based on calibration data given by a free radical reference.

Results

Figure 1 shows the complexes under study as well as their electronic absorption spectra. The lowest-energy absorption band of the title complexes lies between 500 and 550 nm. The band was attributed to the $\sigma \rightarrow \pi^*$ or σ-bond-to-ligand charge transfer (SBLCT) transition from the HOMO (which has σ(Sn−Ru−Me) or σ(Me−Pt−Me) character, respectively) to the π^*(iPr-DAB) LUMO.[1,18]

The FT-EPR spectra of the radicals produced by irradiation of **1H** and **1D** in toluene for delay times of 50 ns and 1 μs are shown in Figure 2. The spectra are assigned to the $CH_3^\bullet$ and $CD_3^\bullet$ radicals on the basis of measured hyperfine splitting constants (hfsc) of 2.27 mT ($CH_3^\bullet$) and 0.33 mT ($CD_3^\bullet$), which are in close agreement with literature values.[27,28] It is noted that the FT-EPR spectra do not show a signal contribution due to the $[Ru(SnPh_3)(CO)_2(iPr\text{-}DAB)]^\bullet$ or $[Pt(Me)_3(iPr\text{-}DAB)]^\bullet$ radicals, probably due to their short T_2 values. This prevents detection of FT-EPR spectra because of the instrument dead time. The g values of the $[M(CO)_3(tBu\text{-}DAB)]^\bullet$ (M = Mn, Re) radicals were found at values (2.0043 and 2.0059, respectively[29]) similar to that of the radical anion of the free ligand (2.0034).[30] The g values of the $[Ru(SnPh_3)(CO)_2(iPr\text{-}DAB)]^\bullet$ or $[Pt(Me)_3(iPr\text{-}DAB)]^\bullet$ radicals are probably similar to those of $[M(CO)_3(tBu\text{-}DAB)]^\bullet$ (M = Mn, Re), because all these complexes are structurally and electronically very similar. This means that the g values of the $[Ru(SnPh_3)(CO)_2(iPr\text{-}DAB)]^\bullet$ or $[Pt(Me)_3(iPr\text{-}DAB)]^\bullet$ radicals are close to those of the $CH_3^\bullet$ and $CD_3^\bullet$ radicals (2.00255). Since for the metal-centered $[Mn(CO)_3(PBu_3)_2]^\bullet$ radical a higher value of 2.030 was found,[31] it was concluded that the odd electron in $[M(CO)_3(tBu\text{-}DAB)]^\bullet$ (M = Mn, Re) is mainly localized on the tBu-DAB ligand.

The $CH_3^\bullet$ and $CD_3^\bullet$ spectra obtained with τ_d = 50 ns show a low-field-emission/high-field-absorption (E/A) CIDEP pattern. In the case of the former radical an additional net emission component is observed (E^*/A), while in the latter a net absorption contribution is present (E/A^*). It is clear that the $CH_3^\bullet$ radical spectrum (Figure 2A) has a much larger signal-to-noise ratio than that of the $CD_3^\bullet$ radical (Figure 2B). Since the photoreactivities of **1H** and **1D** are the same and the spectra were recorded using solutions with similar concentrations, this indicates that the electron polarization generated in the formation of $CH_3^\bullet$ is much larger than that of $CD_3^\bullet$.

As shown in Figure 2 (C, D), at τ_d = 1 μs the spin systems are close to thermal equilibrium. An analysis of the time profiles (not shown) of the intensities of the resonance peaks of the $CH_3^\bullet$ radical in toluene at room temperature shows an exponential decay to thermal equilibrium with a rate constant of 9.5(0.8) × 10^6 s^{-1} corresponding to a spin−lattice relaxation time of 105(13) ns. By comparison, a T_1 measurement of the methyl radical generated by pulse radiolysis in aqueous solution gave a value of 0.2 μs.[32] For the $CD_3^\bullet$ radical a value of 74(40) ns is found. The large uncertainty in this value is due to the relatively poor signal-to-noise, which reflects the absence of strong signal enhancement by CIDEP.

To determine the operative CIDEP mechanisms unambiguously, the solvent effect on the polarization pattern observed in the spectra of the $CH_3^\bullet$ radicals, obtained by irradiation of solutions of **1H** and **2**, was investigated. First the solvent polarity was varied, keeping the viscosity at a similar value. The results are shown in Figure 3, together with the viscosities η (in mPa·s) and relative dielectric constants ϵ_r of the solvents (the latter values are used as indication of solvent polarity). It can be seen that going from toluene to dichloromethane and finally to methanol, i.e., with increasing solvent polarity, the net emission signal contribution to the spectra increases relative to the E/A contribution. When taking into account the dielectric loss due to the solvent on signal intensity, the signal-to-noise ratios of all the spectra are fairly similar.

In contrast, the signal intensity clearly increases upon increasing the solvent viscosity in the case of **2** (Figure 4). The decrease in signal intensity per measurement stays constant, indicating a similar photochemical quantum yield in all solvents. In the case of **1H** a complication arises due to the limited

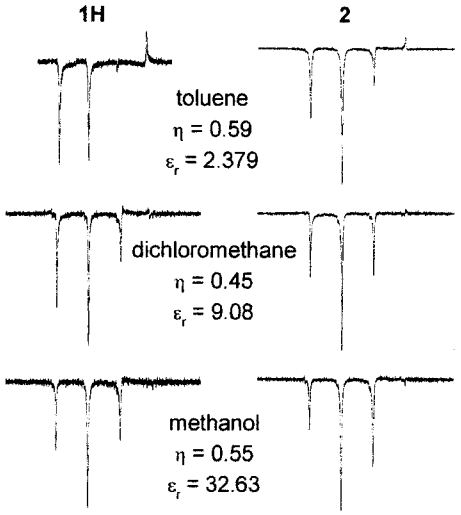

Figure 3. FT-EPR spectra of the methyl radicals produced by photoexcitation (532 nm) of ~1 mM **1H** (left) and **2** (right) in (from top to bottom) toluene, dichloromethane, and methanol at 50 ns delay time. Solvent viscosities, η (in mPa·s), and relative dielectric constants, ϵ_r, are included.

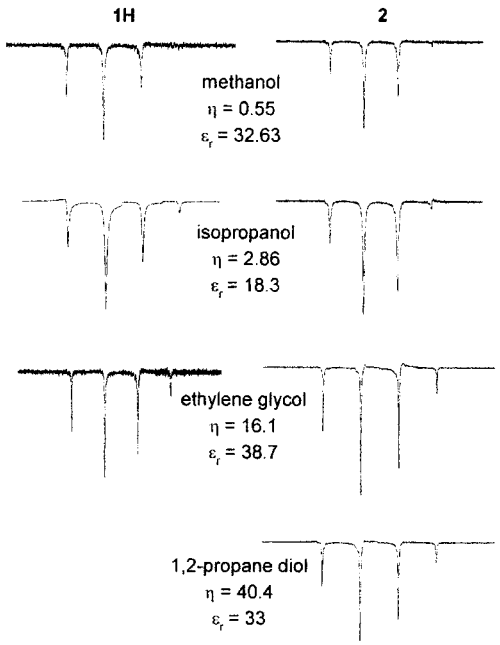

Figure 4. FT-EPR spectra of the methyl radicals produced by photoexcitation (532 nm) of ~1 mM **1H** (left) and **2** (right) in (from top to bottom) methanol, 2-propanol, ethylene glycol, and 1,2-propane diol at 50 ns delay time. Solvent viscosities, η (in mPa·s), and relative dielectric constants, ϵ_r, are included.

solubility of the complex when using ethylene glycol or 1,2-propane diol as solvent. In both systems the length of the free-induction decay (FID) increases, which transforms to narrower lines in the frequency domain. From the increase in signal intensity, it is clear that an increase in solvent viscosity leads to a pronounced increase in a signal contribution stemming from a particular CIDEP mechanism, rather than a decrease of another component. It should be noted that the hyperfine dependent polarization pattern remains unaffected by the strong increase in solvent viscosity, proving that the increased polarization is due to a hyperfine dependent CIDEP mechanism. No strong solvent dependence of the polarization pattern was observed for **1D**, the importance of which will be discussed later.

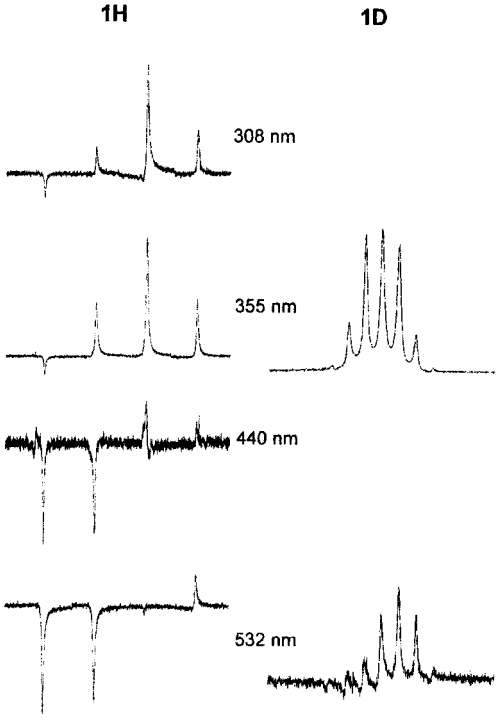

Figure 5. Laser excitation wavelength dependence of the FT-EPR spectra of the methyl radical produced by photoexcitation of **1H** (left) and **1D** (right) dissolved in toluene for a delay time of 50 ns. With 440 nm excitation, signals are the average produced by 4000 laser shots.

Finally, the influence of the excitation wavelength on the polarization pattern was investigated by recording FT-EPR spectra for **1H**, **1D**, and **2**, using 308, 355, 440, and 532 nm irradiation. The surprising results for **1H** and **1D** in toluene are depicted in Figure 5. Excitation at shorter wavelengths leads to a shift in polarization pattern from *E**/*A* to *E*/*A** for **1H** and from *E*/*A** to *A* for **1D**. For the latter complex this shift is accompanied by a large increase in signal intensity. The polarization patterns observed for radicals generated from **1H** using short-wavelength irradiation seem to be less solvent sensitive than those observed using long-wavelength irradiation, since the results for **1H** are virtually the same in methanol and toluene (not shown). In contrast, no influence of the excitation wavelength on the polarization pattern was observed in the case of **2**. In a recent study on the photoinduced reactions of xanthone with alcohols, a slight excitation wavelength dependence of the polarization pattern was observed.[33,34] An earlier example[35] was later disputed.[36]

Discussion

All the recorded FT-EPR spectra in this study display an *E*/*A* pattern to some extent. This is a clear indication that the ST_0 radical pair mechanism (RPM) is operative and that the radicals are formed from a triplet excited state precursor (assuming the sign of the exchange interaction is negative, i.e., the singlet radical pair state is lower in energy than the triplet).[37] In its usual form, this mechanism is a three-step process. After formation of the geminate radical pair, the radicals diffuse apart, which decreases the exchange interaction, allowing the singlet level and the T_0 component of the triplet level to mix through the hyperfine coupling. The magnitude of the polarization created in this way is a function of the difference in resonance frequencies between the two (hyperfine components of the) radicals that form the radical pair.[37,38] The finding that deuteration strongly decreases the polarization magnitude

(cf. Figure 2A,B) establishes that the difference in resonance frequencies must be primarily determined by the hyperfine coupling constant. A comparison of the signal intensities of the spectra from **1D** at short and long delay times (cf. Figure 2) shows that the CIDEP and Boltzmann signals are of similar magnitude. Given the short T_1, this means that the observed intensity pattern in the spectrum for **1D** (Figure 2B) can be satisfactorily explained by a combination of Boltzmann and ST_0 RPM signal contributions.

As shown in Figure 3, an increase in solvent polarity leads to a decrease in polarization due to the ST_0 RPM in the spectra of **1H** and **2** (cf. Figure 3). Apparently, the more polar solvents can cause the radical pair to break up at some point before the final reencounter step of the ST_0 RPM. Upon increase of the solvent viscosity, in polar solvents where the ST_0 RPM signal contribution is small, the net emissive signal contribution is strongly enhanced for **1H** and **2** (cf. Figure 4), but not for **1D.** This suggests that this contribution is due to a CIDEP mechanism in which the polarization is generated by hyperfine interaction as well. The contribution is attributed to the ST_{-1} RPM,[37,39,40] in which the singlet level interacts with the T_{-1} component of the triplet level, rather than with the T_0 component. This one-step mechanism is generally only operative in cases of high solvent viscosity and/or large hyperfine interaction. This mechanism generates a net emissive spectrum with stronger polarization in the low field than in the high field part of the spectrum. Exactly this pattern is observed when employing a very high viscosity solvent (Figure 4). The operation of this mechanism in a polar solvent suggests also that the ST_0 RPM contribution is diminished due to prevention of the reencounter step rather than more rapid breakup of the geminate radical pair.

The triplet mechanism (TM), which is often invoked to explain net polarization patterns, could in principle also give rise to the observed net emission contribution in the spectra of **1H** and **2**. In this mechanism, spin polarization is created through spin-selective intersystem crossing (ISC) from the singlet to the triplet excited state.[37,41] This polarization is then transferred to the radicals. The magnitude of the hyperfine independent TM polarization depends on solvent viscosity and reaction rate.[41,42] An increase in viscosity increases the rotational correlation time, leading to a larger spin polarization. Apart from the hyperfine dependence of the polarization pattern, this matches our experimental observations. For TM CIDEP to make a significant signal contribution, the reaction rate (k_r) should be large enough to compete with the rate of spin−lattice relaxation of the triplet, which typically is $\geq 10^9$ s^{-1}. On the other hand, if the reaction rate is fast compared to the electron spin Larmor frequency, $k_r > \omega_0$, spin-selective ISC does not give rise to TM CIDEP.[42] There are indications that the photochemical reaction rate is indeed very high. First, the observed photochemical quantum yield of ca. 0.5 is temperature independent and excitation wavelength dependent throughout the lowest-energy absorption band.[6] This suggests that the photochemical reaction is an activationless process in competition with vibrational relaxation.[43] Second, for a related complex, [Re(Me)$(CO)_3$(dmb)] (dmb = 4,4′-dimethyl-2,2′-bipyridine), the excited state lifetime was experimentally determined to be shorter than 400 fs.[44] Several other examples of ultrafast photochemical reactions in organometallic chemistry have been reported in the literature.[9,45−49] A final argument against a TM contribution is the fact that the solvent viscosity has no influence on the polarization pattern in the case of **1D**. This would be expected if the hyperfine independent TM were operative (vide supra).

The excitation wavelength dependence of the polarization pattern found for **1H** and **1D** (cf. Figure 5) can also be explained by the fact that optical excitation is followed by a reaction from thermally nonequilibrated excited states (a so-called prompt chemical reaction). As noted before, the lowest-energy absorption band of **1** and related complexes has been assigned to a σ(Sn−Ru−Me) → π^*(iPr-DAB) (SBLCT) transition on the basis of the resonance Raman and time-resolved IR spectra and DFT MO calculations on model complexes such as [Ru(SnH_3)(Me)$(CO)_2$(H-DAB)]. According to these calculations the σ(Sn−Ru−Me) HOMO is a delocalized orbital, which consists of contributions from p_x(Ru), the antisymmetric sp^3(Sn)−sp^3(Me) combination, and π^*(H-DAB).[18] Similarly, the first electronic transition of **2** is the σ(Me−Pt−Me) → π^*(iPr-DAB) (SBLCT) transition.[1] The second electronic transition of complexes **1** and **2** found at 388 nm for **1H** and at 326 nm for **2** (in toluene, cf. Figure 1) belongs to a d_π(Ru, Pt) → π^*(iPr-DAB) (MLCT) transition.[1,18] In contrast with the SBLCT state, this MLCT state is not reactive and MLCT excitation will result in radical formation only via occupation of the lower lying reactive SBLCT state. In agreement with this, irradiation of **2** into its second absorption band with 308 or 355 nm results in exactly the same polarization pattern as found upon 440 or 532 nm excitation.

In the case of **1H**, 440 and 532 nm excitation again gives rise to the same polarization pattern. With the available setup irradiation of **1H** into its second absorption (MLCT) band at 388 nm was not possible. Surprisingly, the use of 355 nm excitation gave rise to a polarization pattern different from that observed at 440 and 532 nm, but exactly similar to that found upon 308 nm irradiation. Apparently, the radicals formed on 355 nm excitation are not produced from the lowest SBLCT state via MLCT excitation as for **2**. In view of the close similarity of the polarization patterns, the radicals obtained by 355 and 308 nm excitation are most likely both produced from a thermally nonequilibrated excited state at higher energy.

A likely candidate for this higher lying excited state is the second SBLCT state. According to DFT MO calculations, the model complex [Ru$(SnH_3)_2(CO)_2$(H-DAB)][50] has indeed a second σ'(Sn−Ru−Sn) orbital, consisting of contributions from d_{x^2}(Ru) and the symmetric sp^3(Sn)+sp^3(Sn) combination. A second SBLCT transition, i.e., σ'(Sn−Ru−Sn) → π^*(H-DAB) will originate from this orbital and is expected to be ca. 2 eV higher in energy than the first SBLCT transition. The first SBLCT transition lies at 531 nm for **1**, and hence the second SBLCT transition should be at about 300 nm for **1**. This second SBLCT state will also be reactive, and the different polarization patterns in the FT-EPR spectra of **1** are therefore attributed to the formation of radicals by prompt chemical reaction from the two different SBLCT states. In the case of **2**, the energy difference between the two σ(Me−Pt−Me) orbitals is expected to be much larger (3.3 eV), according to preliminary DFT MO calculations of [Pt$(Me)_4$(iPr-DAB)].[51] This should position the second SBLCT transition at about 220 nm, which explains the absence of any wavelength effect for **2**.

The above explanation is supported by the absence of any wavelength dependence of the CIDEP pattern in the case of the related complexes [Ru(I)(iPr)$(CO)_2$(iPr-DAB)] and [Re(R)$(CO)_3$(4,4′-dimethyl-2,2′-bipyridine)] (R = Et, iPr).[3] These complexes have only a single σ(M−R) bond and therefore only one low-lying SBLCT state from which radicals are formed.

For both **1H** and **1D** a strong increase in absorptive contribution to the CIDEP pattern is observed on short-wavelength irradiation, suggesting that this additional component is due to a hyperfine independent mechanism. Apart from the TM, one other hyperfine independent mechanism is known: the

spin−orbit coupling induced polarization mechanism (SOCM).[52,53] This mechanism involves spin-selective back reaction from a triplet contact radical pair to the singlet ground state, which leads to selective depopulation of certain triplet sublevels. However, since this mechanism is independent of the excitation wavelength, it is unlikely to be operative.

Conclusion

Numerous studies dealing with spin selectivity of photochemical reactions involving transition metal complexes have been published in recent years.[54,55] Most of these papers deal with magnetic field effects on reaction dynamics, and very few are concerned with applications of time-resolved EPR. The results presented here and in previous work[2,19,20] show that investigations with time-resolved EPR techniques can contribute to the understanding of the mechanisms of photochemical reactions involving transition metal complexes.

Acknowledgment. Financial support for this work was provided by the Division of Chemical Sciences, Office of Basic Energy Sciences of the U.S. Department of Energy (DE-FG02-84ER-13242), and the Council for Chemical Sciences of the Netherlands Organization for Scientific Research (CW-NWO).

References and Notes

(1) Kaim, W.; Klein, A.; Hasenzahl, S.; Stoll, H.; Záliš, S.; Fiedler, J. *Organometallics* **1998**, *17*, 237.
(2) Kleverlaan, C. J.; Stufkens, D. J.; Clark, I. P.; George, M. W.; Turner, J. J.; Martino, D. M.; van Willigen, H.; Vlček, A., Jr. *J. Am. Chem. Soc.* **1998**, *120*, 10871.
(3) Rossenaar, B. D.; Kleverlaan, C. J.; van de Ven, M. C. E.; Stufkens, D. J.; Vlček, A., Jr. *Chem. Eur. J.* **1996**, *2*, 228.
(4) Rossenaar, B. D.; George, M. W.; Johnson, F. P. A.; Stufkens, D. J.; Turner, J. J.; Vlček, A., Jr. *J. Am. Chem. Soc.* **1995**, *117*, 11582.
(5) Kleverlaan, C. J.; Stufkens, D. J. *J. Photochem. Photobiol. A: Chem.* **1998**, *116*, 109.
(6) Aarnts, M. P.; Stufkens, D. J.; Vlček, A., Jr. *Inorg. Chim. Acta* **1997**, *266*, 37.
(7) Rossenaar, B. D.; Stufkens, D. J.; Oskam, A.; Fraanje, J.; Goubitz, K. *Inorg. Chim. Acta* **1996**, *247*, 215.
(8) Bradley, P.; Suardi, G.; Zipp, A. P.; Eisenberg, R. *J. Am. Chem. Soc.* **1994**, *116*, 2859.
(9) Walker, L. A., II; Jarrett, J. T.; Anderson, N. A.; Pullen, S. H.; Matthews, R. G.; Sension, R. J. *J. Am. Chem. Soc.* **1998**, *120*, 3597.
(10) Pourreau, D. B.; Geoffroy, G. L. *Adv. Organomet. Chem.* **1985**, *24*, 249.
(11) Kaupp, M.; Stoll, H.; Preuss, H.; Kaim, W.; Stahl, T.; van Koten, G.; Wissing, E.; Smeets, W. J. J.; Spek, A. L. *J. Am. Chem. Soc.* **1991**, *113*, 5606.
(12) Hasenzahl, S.; Kaim, W.; Stahl, T. *Inorg. Chim. Acta* **1994**, *225*, 23.
(13) Guilard, R.; Mitaine, P.; Moïse, C.; Lecomte, C.; Boukhris, A.; Swistak, C.; Tabard, A.; Lacombe, D.; Cornillon, J.-L.; Kadish, K. M. *Inorg. Chem.* **1987**, *26*, 2467.
(14) Hageman, H. J. *Prog. Org. Coat.* **1985**, *13*, 123.
(15) Udding, J. H.; Giesselink, J. P. M.; Hiemstra, H.; Speckamp, W. N. *J. Org. Chem.* **1994**, *59*, 6671.
(16) Yang, D. B.; Kutal, C. *Inorganic and Organometallic Photoinitiators*; Pappas, S. P., Ed.; Plenum Press: New York, 1992; pp 21−55.
(17) Nieuwenhuis, H. A.; van de Ven, M. C. E.; Stufkens, D. J.; Oskam, A.; Goubitz, K. *Organometallics* **1995**, *14*, 780.
(18) Aarnts, M. P.; Stufkens, D. J.; Wilms, M. P.; Baerends, E. J.; Vlček, A., Jr.; Clark, I. P.; George, M. W.; Turner, J. J. *Chem. Eur. J.* **1996**, *2*, 1556.
(19) Kleverlaan, C. J.; Martino, D. M.; van Willigen, H.; Stufkens, D. J.; Oskam, A. *J. Phys. Chem.* **1996**, *100*, 18607.
(20) Sakaguchi, Y.; Hayashi, H.; l'Haya, Y. J. *J. Phys. Chem.* **1990**, *94*, 291.
(21) Kleverlaan, C. J.; Martino, D. M.; van Slageren, J.; van Willigen, H.; Stufkens, D. J.; Oskam, A. *Appl. Magn. Reson.* **1998**, *15*, 203.
(22) Aarnts, M. P.; Stufkens, D. J.; Oskam, A.; Fraanje, J.; Goubitz, K. *Inorg. Chim. Acta* **1997**, *256*, 93.
(23) Hasenzahl, S.; Hausen, H.-D.; Kaim, W. *Chem. Eur. J.* **1995**, *1*, 95.
(24) Levstein, P. R.; van Willigen, H. *J. Chem. Phys.* **1991**, *95*, 900.
(25) van Willigen, H.; Levstein, P. R.; Ebersole, M. H. *Chem. Rev.* **1993**, *93*, 173.
(26) de Beer, R.; van Ormondt, D. *Advanced EPR: Applications in Biology and Biochemistry*; Elsevier: Amsterdam, 1989.
(27) Sullivan, P. D.; Koski, W. S. *J. Am. Chem. Soc.* **1962**, *84*, 1.
(28) Fessenden, R. W.; Schuler, R. H. *J. Chem. Phys.* **1963**, *39*, 2147.
(29) Andréa, R. R.; de Lange, W. G. J.; van der Graaf, T.; Rijkhoff, M.; Stufkens, D. J.; Oskam, A. *Organometallics* **1988**, *7*, 1100.
(30) tom Dieck, H.; Kühl, E. *Z. Naturforsch. B* **1982**, *37*, 324.
(31) Kidd, D. R.; Cheng, C. P.; Brown, T. L. *J. Am. Chem. Soc.* **1978**, *100*, 4103.
(32) Bartels, D. M.; Lawler, R. G.; Trifunac, A. D. *J. Chem. Phys.* **1985**, *83*, 2686.
(33) Koga, T.; Ohara, K.; Kuwata, K.; Murai, H. *J. Phys. Chem. A* **1997**, *101*, 8021.
(34) Ohara, K.; Hirota, N.; Martino, D. M.; van Willigen, H. *J. Phys. Chem. A* **1998**, *102*, 5433.
(35) Khudyakov, I. V.; McGarry, P. F.; Turro, N. J. *J. Phys. Chem.* **1993**, *97*, 13234.
(36) Meng, Q.-X.; Sakaguchi, Y.; Hayashi, H. *Mol. Phys.* **1997**, *90*, 15.
(37) McLauchlan, K. A. *Continuous-Wave Transient Electron Spin Resonance CIDEP*; Kevan, L., Bowman, M. K., Eds.; Wiley: New York, 1990; pp 285−363.
(38) Monchik, L.; Adrian, F. J. *J. Chem. Phys.* **1978**, *68*, 4376.
(39) Buckley, C. D.; McLauchlan, K. A. *Chem. Phys. Lett.* **1987**, *137*, 86.
(40) Trifunac, A. D. *Chem. Phys. Lett.* **1977**, *49*, 457.
(41) Ces, O.; McLauchlan, K. A.; Qureshi, T. J. J. *Appl. Magn. Reson.* **1997**, *13*, 297.
(42) Atkins, P. W.; Evans, G. T. *Mol. Phys.* **1974**, *27*, 1633.
(43) Langford, C. H. *Acc. Chem. Res.* **1984**, *17*, 96.
(44) Farrell, I. R.; Matousek, P.; Kleverlaan, C. J.; Vlček, A., Jr. *Chem. Eur. J.*, in press.
(45) Shiang, J. J.; Walker, L. A., II; Anderson, N. A.; Cole, A. G.; Sension, R. J. *J. Phys. Chem. B* **1999**, *103*, 10532.
(46) Lindsay, E. M.; Langford, C. H.; Kirk, A. D. *Inorg. Chem.* **1999**, *38*, 4771.
(47) Lindsay, E.; Vlček, A., Jr.; Langford, C. H. *Inorg. Chem.* **1993**, *32*, 2269.
(48) Farrell, I. R.; Matousek, P.; Vlček, A., Jr. *J. Am. Chem. Soc.* **1999**, *121*, 5296.
(49) Víchová, J.; Hartl, F.; Vlček, A., Jr. *J. Am. Chem. Soc.* **1992**, *114*, 10903.
(50) Aarnts, M. P.; Wilms, M. P.; Peelen, K.; Fraanje, J.; Goubitz, K.; Hartl, F.; Stufkens, D. J.; Baerends, E. J.; Vlček, A., Jr. *Inorg. Chem.* **1996**, *35*, 5468.
(51) Záliš, S. Personal communication, 2000.
(52) Katsuki, A.; Akiyama, K.; Tero-Kubota, S. *Bull. Chem. Soc. Jpn.* **1995**, *68*, 3383.
(53) Katsuki, A.; Akiyama, K.; Ikegami, Y.; Tero-Kubota, S. *J. Am. Chem. Soc.* **1994**, *116*, 12065.
(54) Steiner, U. E.; Ulrich, T. *Chem. Rev.* **1989**, *89*, 51.
(55) Khudyakov, I. V.; Serebrennikov, Y. A.; Turro, N. J. *Chem. Rev.* **1993**, *93*, 537.